Journal of Intelligent Material Systems and Structures
http://jim.sagepub.com/

Dynamic Characteristics of ER Fluid-filled Composite Plate using Multielectrode Configuration

Ki-Dae Cho, In Lee and Jae-Hung Han

Journal of Intelligent Material Systems and Structures 2005 16: 411
DOI: 10.1177/1045389X05051002

The online version of this article can be found at:
http://jim.sagepub.com/content/16/5/411

Published by:
SAGE
http://www.sagepublications.com

Dynamic Characteristics of ER Fluid-filled Composite Plate using Multielectrode Configuration

KI-DAE CHO, IN LEE AND JAE-HUNG HAN*

Department of Aerospace Engineering, Korea Advanced Institute of Science and Technology 373-1 Guseong-dong, Yuseong-gu, Daejeon 305-701, Korea

ABSTRACT: In this research, a smart structure with multielectrode configuration has been proposed, which contains electrorheological (ER) fluid. Multielectrode configuration gives the structure a capability to change its modal characteristics effectively. The proposed configuration also provides the effective vibration control performance with reduced power consumption in the smart structures. A finite element model has been developed for the analysis of a smart composite plate under fully and partially applied electric fields. The numerical results of the composite plate with ER fluid have been compared with the experimental results. The performance and energy consumption of the control system have been experimentally investigated for various applied areas of electric field by applying a semi-active control law to the vibrating composite plate.

Key Words: smart composite plate, electrorheological (ER) fluid, vibration suppression, finite element analysis, semi-active control

INTRODUCTION

MANY experimental and theoretical studies for smart structures containing electrorheological (ER) fluids have been carried out ever since Winslow first discovered the controllability of the rheological property by the applied electric field in 1949. Gandhi et al. (1989) suggested the possibility of using ER fluids to suppress deflections of the ER fluid-based structures by avoiding resonance situation. Choi et al. (1990) studied the vibration characteristics of an ER beam. Several researchers have introduced the conventional sandwich beam theories (Ross et al., 1959; Mead and Markus, 1969) to formulate an analytical model for the ER fluid-filled structures. Yalcintas and Coulter (1995) examined the applicability of two theoretical structural theories, the RKU model (Ross et al., 1959) and the Mead and Markus model (Mead and Markus, 1969), originally developed for polymer-based beam structures, to ER-based beam structures. Rahn and Joshi (1998) performed numerical simulation of vibration control of ER sandwich beams, but the experimental implementation realizing an active vibration control was not accomplished. Choi et al. (1999) used a finite element model based on the three-layer model by Mead and Markus (1969) to predict field-dependent modal characteristics of an ER fluid-based plate with four partitioned electrodes. The analysis results were also compared with their experimental observations. Electrode segmentation was also applied to piezoelectric actuators for the control performance improvement (Han and Lee, 1997).

This study investigates the dynamic modeling and vibration characteristics of ER fluid-filled plate structure using refined multielectrode configurations. The effects of active electrodes on the vibration characteristics of the multilayer composite plate with embedded ER fluid are studied through refined finite element analysis and experiment for both passive and semi-active operational modes of ER fluids.

FINITE ELEMENT FORMULATION

This section describes finite element formulations for a multilayer composite plate containing ER fluids. Generally, the constitutive behaviors of the ER fluid can be divided into pre-yield and post-yield regions. With the small amplitude vibration, it can be assumed that the ER fluid remains in the pre-yield region, where the complex shear modulus of the ER fluid can be controlled by the applied electric field. Therefore, the finite element procedures applied for the laminated plates with viscoelastic damping layers can be used with minimum modification to analyze composite plates containing ER fluids.

Based on the layerwise plate theory (Reddy, 1987), the displacement fields (u, v, w) for a two-dimensional

*Author to whom correspondence should be addressed.
E-mail: jaehunghan@kaist.ac.kr

1045-389X/05/05 0411–9 $10.00/0 DOI: 10.1177/1045389X05051002

element i, of which the area is defined as Ω_i can be expressed by introducing the through-the-thickness piecewise interpolation function, $\Phi^J(z)$.

$$u = \sum_{J=1}^{N_i} U^J(x,y,t)\Phi^J(z), \quad v = \sum_{J=1}^{N_i} V^J(x,y,t)\Phi^J(z) \quad (1)$$
$$w = W(x,y,t)$$

Here (U^J, V^J, W) are undetermined coefficients for in-plane displacements and N_i is the number of degrees of freedom for the in-plane displacement through the thickness for element i. The linear strain–displacement relation is adopted and constitutive equations of the kth layer can be written as:

$$\{\sigma\}_k = [\overline{C}]\{\varepsilon\}_k \quad (2)$$

where $[\overline{C}]$ is the transformed reduced stiffness matrix. The constitutive equation in the geometric x–y–z coordinate system can be obtained by the proper coordinate transformation. Note that the stiffness of the ER fluid is a function of the applied electric field, excitation frequency, and the strain amplitude.

In order to derive the equation of motion for the ER fluid-based laminated plate, Hamilton's principle was applied. Integration of the combined equation of Equations (1) and (2), and well-known strain–displacement relationship through the thickness of the ER fluid-based laminated plate provides the following equation of motion:

$$\int_0^T\int_{\Omega_i}\Bigg[\delta\mathbf{e}^T\mathbf{A}_\mathrm{S}\mathbf{e} + \sum_J^{N_i}\left\{\delta\mathbf{e}^T\mathbf{B}_\mathrm{S}^J\mathbf{e}_\mathrm{S}^J + \delta\mathbf{e}_\mathrm{S}^{J^T}\mathbf{B}_\mathrm{S}^J\mathbf{e}\right\} + \sum_J^{N_i}\sum_K^{N_i}\left\{\delta\mathbf{e}^{J^T}\mathbf{D}^{JK}\mathbf{e}^K + \delta\mathbf{e}_\mathrm{S}^{J^T}\mathbf{D}_\mathrm{S}^{JK}\mathbf{e}_\mathrm{S}^K\right\} + I^0\delta W\ddot{W} + \sum_J^{N_i}\sum_K^{N_i}\delta\mathbf{d}^{J^T}\mathbf{I}^{JK}\ddot{\mathbf{d}}^K\Bigg]dA\,dt = 0 \quad (3)$$

where δ and $\ddot{(\,)}$ mean the variational operator and the second differentiation with respect to time, respectively, and the subscript S denotes transverse shear properties, and the other symbols can be referred from Cho et al. (2000).

Introducing Lagrangian shape functions, the finite element formulation of the ER fluid-based laminated plate in sinusoidal motion gives the equation of motion in the form of a standard eigenvalue problem for free vibration analysis:

$$(\mathbf{K} - \omega^2\mathbf{M})\mathbf{u} = 0 \quad (4)$$

where $\mathbf{M}$ and $\mathbf{K}$ are the global mass and stiffness matrices, respectively; $\mathbf{u}$ is the nodal displacement vector of the whole system and ω is the natural frequency.

The modal damping based on the modal strain energy (MES) method of the ER fluid-based laminated plate is defined as:

$$\eta = \frac{1}{2\pi}\frac{\Delta E}{E} \quad (5)$$

where ΔE is the energy dissipated per cycle and E is the maximum strain energy. The dissipated energy can be expressed as:

$$\Delta E_e = \frac{1}{2}\int_{\Omega_i}\Bigg[\mathbf{e}^T\hat{\mathbf{A}}_\mathrm{S}\mathbf{e} + \sum_J^{N_i}\{\mathbf{e}^T\hat{\mathbf{B}}_\mathrm{S}^J\mathbf{e}_\mathrm{S}^J + \mathbf{e}_\mathrm{S}^{J^T}\hat{\mathbf{B}}_\mathrm{S}^J\mathbf{e}\} + \sum_J^{N_i}\sum_K^{N_i}\{\mathbf{e}^{J^T}\hat{\mathbf{D}}^{JK}\mathbf{e}^K + \mathbf{e}_\mathrm{S}^{J^T}\hat{\mathbf{D}}_\mathrm{S}^{JK}\mathbf{e}_\mathrm{S}^K\}\Bigg]dA \quad (6)$$

Since $\hat{\mathbf{A}}_\mathrm{S}$, $\hat{\mathbf{B}}_\mathrm{S}^J$, $\hat{\mathbf{D}}^{JK}$, and $\hat{\mathbf{D}}_\mathrm{S}^{JK}$ are the damped stiffness matrices as documented well in Cho et al. (2000), the details are omitted here. The dissipated energy can be obtained by the introduction of Lagrangian shape functions as follows:

$$\Delta E = \sum_{\mathrm{e}=1}^{Ne}\Delta E_e = \frac{1}{2}\mathbf{u}^T\mathbf{K}_\mathrm{d}\mathbf{u} \quad (7)$$

where $\mathbf{K}_\mathrm{d}$ is the total damped stiffness matrix. In the computation of stiffness matrix, the reduced integration is used for the terms related to shear dissipation energy.

Therefore, the loss factor for each mode based on the MSE method can be computed as:

$$\eta_i = \frac{1}{2\pi}\frac{\Delta E_i}{E_i} = \frac{1}{2\pi}\frac{\phi_i^T\mathbf{K}_\mathrm{d}\phi_i}{\phi_i^T\mathbf{K}\phi_i} \quad (8)$$

where ϕ_i is the ith modal vector obtained from the free vibration analysis.

FABRICATION OF SMART COMPOSITE PLATE

The ER fluid-filled smart plate is fabricated by sandwiching an ER fluid between two faceplates and sealing with a silicone rubber. The faceplate consists of a glass–epoxy laminate with the layups of $[0_4]_T$ as a host structural member and a copper-clad laminate as an electrode. A copper-clad laminate is in such a form that one side of a glass–epoxy woven laminate is coated with a very thin copper layer. The copper-clad laminate used in the lower faceplate serves as an electrode of common electric field. The copper-clad laminate used in the upper faceplate has a multielectrode configuration to provide different electric fields to the ER fluid domain independently. The printed circuit technology is used to make this configuration. First, the negative image of the multielectrode configuration designed in full scale is

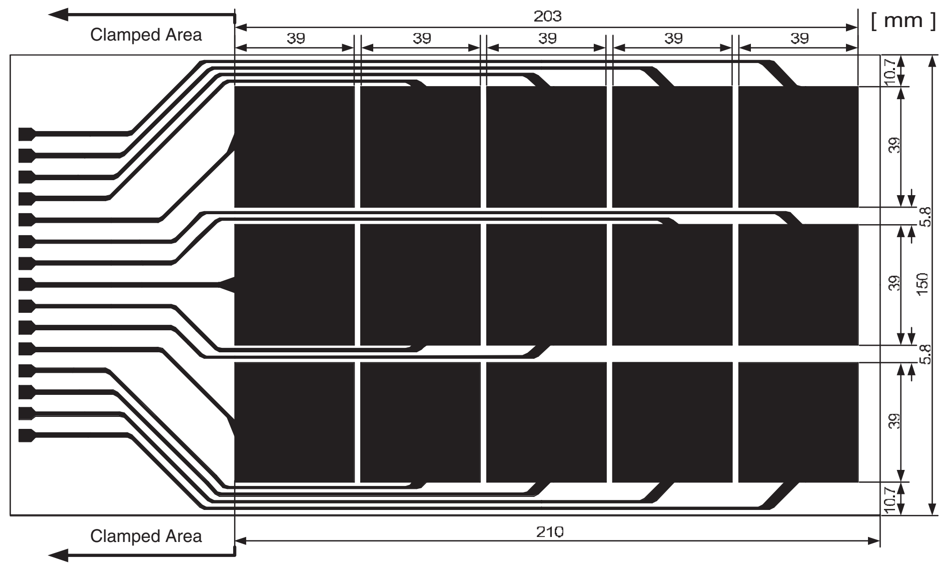

Figure 1. *Configuration of positive multielectrode.*

printed on a negative film as shown in Figure 1. Then, a photosensitizer is applied over the entire surface of the copper-clad laminate and dried in a temperature-controlled oven. After being exposed to light through the negative image, the copper-clad laminate is developed to leave a protective coating on the multielectrode configuration. The exposed area is chemically etched out using ferric chloride as the etch. Consequently, it changes the surface of the copper-clad laminate into the multielectrode configuration, where the copper layer is partitioned into 5×3 segments. This procedure is illustrated in Figure 2. Each faceplate is prepared by joining each electrode sheet made by applying printed circuit technology to a glass–epoxy laminate with cyanoacrylate adhesive.

The silicone rubber strips that serve as the electrical insulators between the two faceplates are lined up along the free edges of the upper faceplate. At the clamped end of the smart plate, a glass–epoxy pad is bonded as the midlayer to provide both insulation and rigidity against the clamping force. The lower faceplate is bonded to the silicone rubber strips with liquid silicone adhesive (Loctite LC-1524). After this, the hollow sandwich plate is exposed to room temperature and is filled with ER fluid. Piezoceramic actuator is bonded to the surface of the upper faceplate to obtain steady-state responses. The constructed smart plate is presented in Figure 3.

DYNAMIC CHARACTERISTICS

Experimental Implementation

Figure 4 presents an experimental apparatus to investigate the dynamic characteristics of the smart plate. The cantilevered plate was clamped in the fixture. Each electrode terminal in the upper faceplate was wired to a switch box in such a way that each can be connected separately to the positive potential, while the common electrode in the lower faceplate was connected to the negative potential of a high voltage electric power supply (Matsusada, HEOPS-5B6).

The characteristics of a smart plate can be obtained by modal testing techniques. In this study, the actuation force can be given by both the impact hammer (PCB 086B01) and the bonded piezoelectric actuator. As a measuring device, a laser displacement meter (Keyence LB-1001) was used. The output from the impact hammer and the laser sensor were connected to an FFT analyzer (HP 3567A) to measure the frequency response function. The frequency response functions were then transferred to the STAR modal software system, and they were curve fitted using a polynomial function to obtain the natural frequencies and damping ratios. The bonded piezoelectric actuator was used to apply steady-state responses in the time domain under forced excitation.

Identification of Dynamic Characteristics

The smart composite plate has a dimension of $210 \times 150 \times 2.41\,\text{mm}^3$. In the analysis, four node isoparametric elements with 11×10 mesh are used. Each electrode segment was typically modeled using four-plate elements, which provides the sufficient resolution of shear in the ER fluid. For the finite element model depicted in Figure 5, the smart plate was treated as three sublaminates when assigning through-the-thickness degrees of freedom. No additional degrees of freedom are assigned to the individual layer in the face sheet for

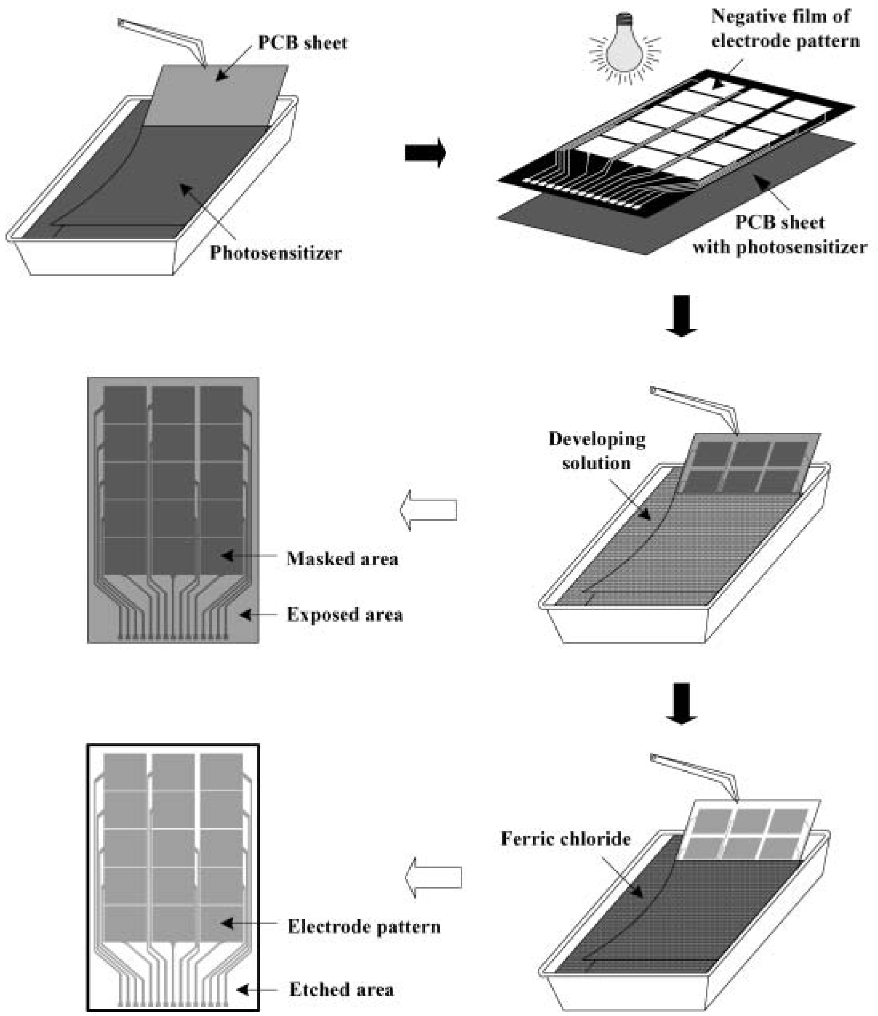

Figure 2. *Schematic procedure for multielectrode shaping.*

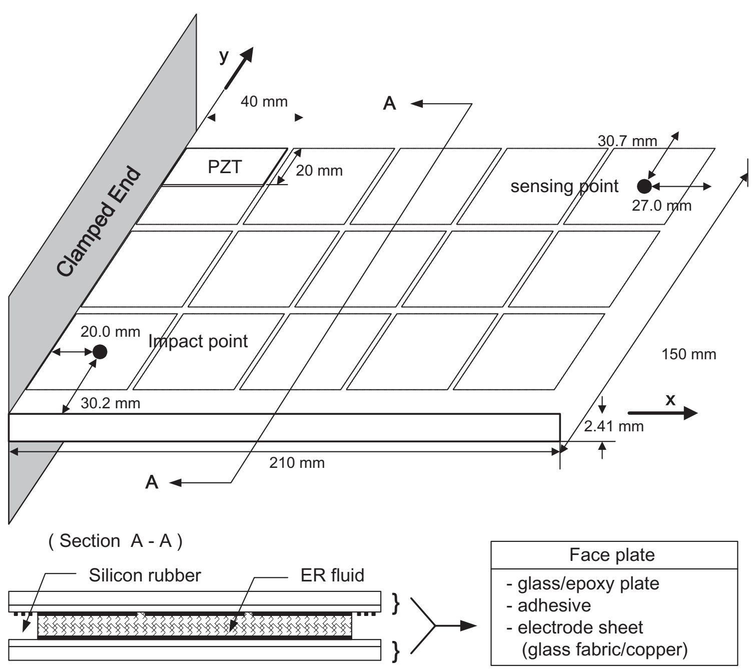

Figure 3. *Configurations for cantilevered ER plate.*

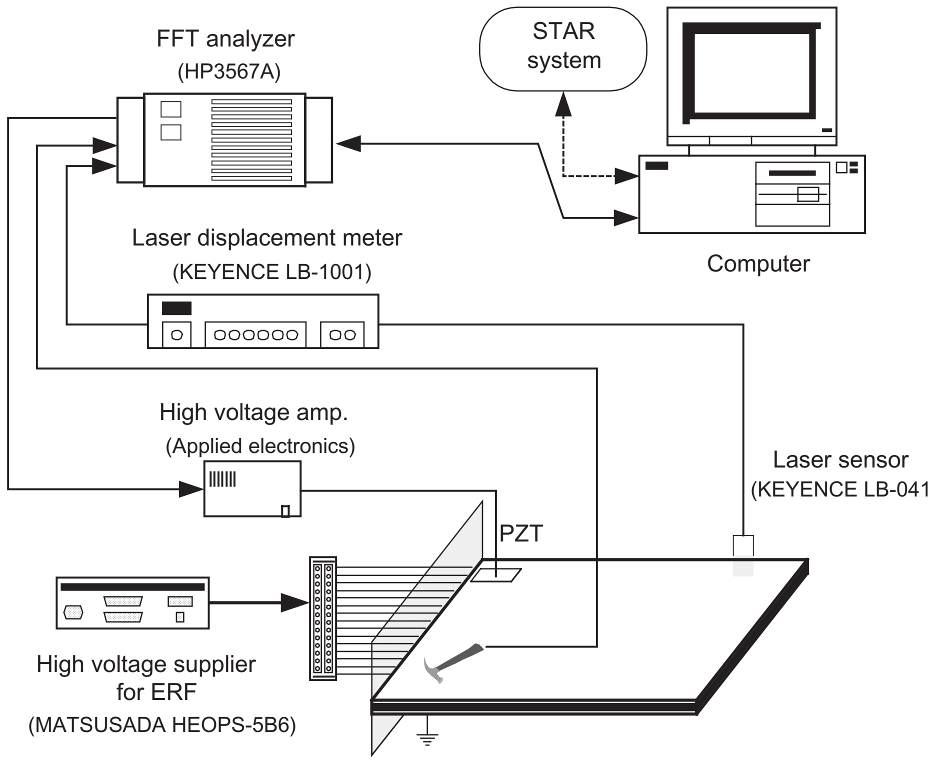

Figure 4. *Experimental setup.*

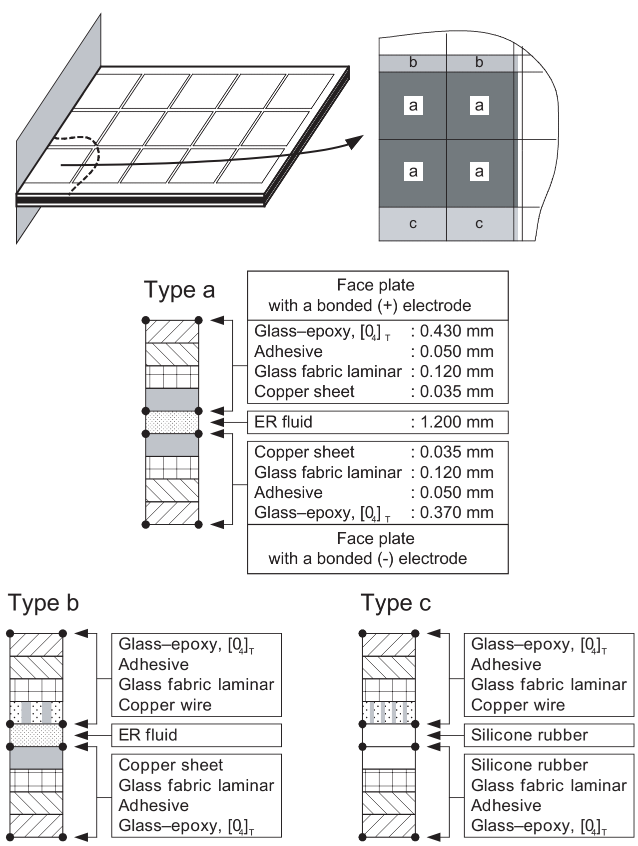

Figure 5. *Finite element model with three sublaminates through the thickness.*

the description of the variable in-plane displacement through the thickness. Table 1 gives the material properties of the faceplate and sealing layer. In the analysis, the effect of the sealing layer on the dynamic properties of the smart plate was considered. The ER fluid used in this study is TX-ER8 of Nippon Shokubai. The rotary oscillation test with ARES rheometer (Rheometric Scientific Inc.) was undertaken to extract the field-dependent complex shear modulus of the ER fluid. The measured values were obtained from ER fluid placed in circular parallel plate fixtures with a diameter of 25 mm, maintaining the gap between the fixtures to be 0.5 mm, under a constant electric field. Figure 6 illustrates the measured storage shear modulus and shear loss factor of the employed ER fluid, which are dependent upon the applied electric field as well as the shear strain. Because the actual strain experienced by an ER fluid layer in the smart plate was controlled to be small, the average values to the extent of a strain rate of 0.1% were used in the analysis. Figure 7 shows the field-dependent complex shear modulus of the ER fluid with a strain of 0.1% with respect to the excitation frequency. However, the modulus and loss factor of the ER fluid used in this experiment can be assumed to be constant near the specific mode, and the material properties at the frequency were used in the analysis.

Table 2 presents the comparison of the numerical predictions and experimental results for the natural

Table 1. Material properties of the faceplate and silicone rubber.

	Face plate				Silicone rubber
			Electrode sheet		
	Glass–epoxy	Adhesive	Glass–fabric	Copper	
E_L (GPa)	43.5	1.78	19.6	120	4.47e−4
E_T (GPa)	5.0	1.78	19.6	120	4.47e−4
G_{LT} (GPa)	5.0	0.69	4.5	44	1.5e−4
ν_{LT}	0.25	0.3	0.17	0.35	0.49
ρ (kg/m^3)	1980	1050	1994	8980	1500
η_{mn} (%)	0.524	0.782	0.804	0.518	11.3
η_{ms} (%)	0.572	0.782	1.441	0.518	11.3

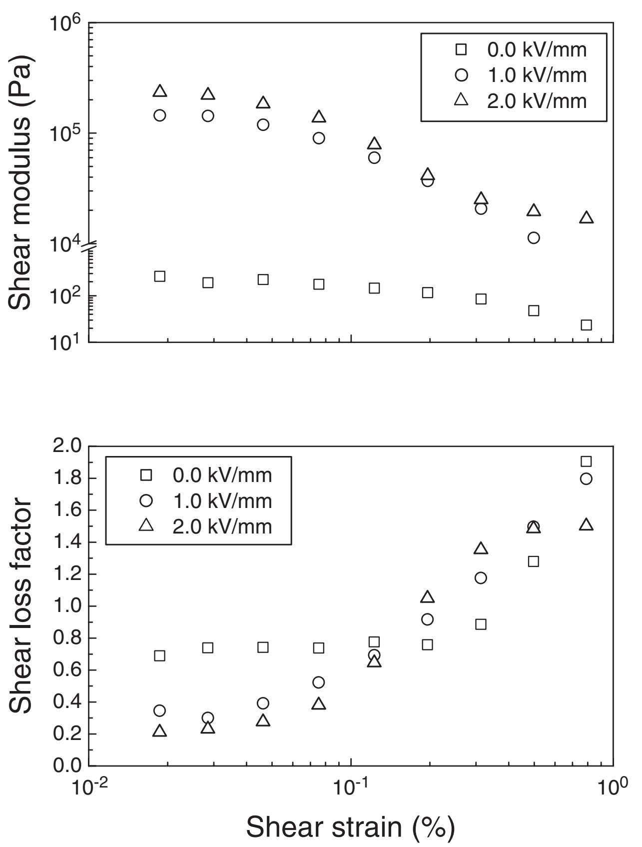

Figure 6. *Field-dependent complex shear modulus of the ER fluid with respect to strain.*

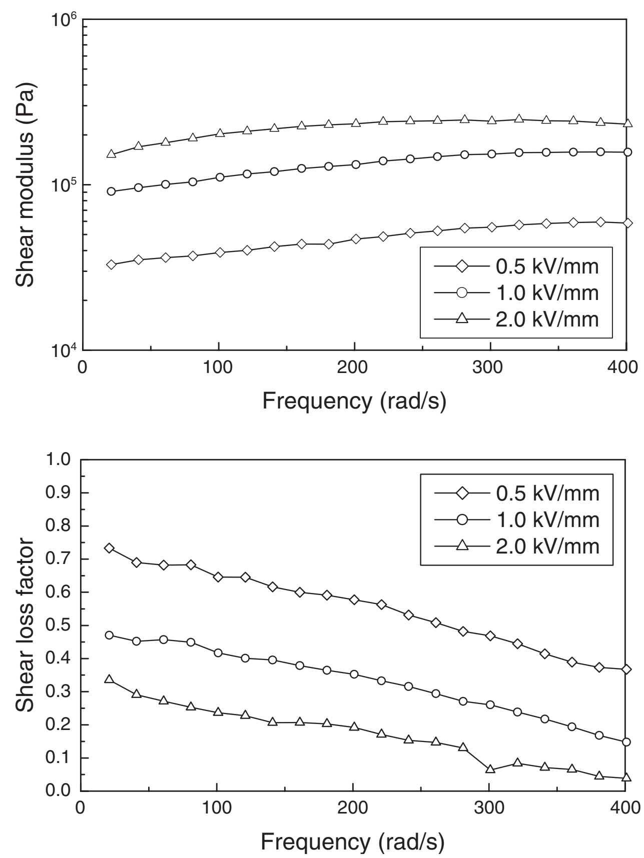

Figure 7. *Field-dependent complex shear modulus of the ER fluid with respect to frequency.*

frequency and loss factor for the fundamental mode of the plate when it is subjected to an electric field of 1 kV/mm. The effects of electrode patterns on the dynamic characteristics of the plate were studied. The predicted fundamental frequency and loss factor are in good agreement with the experimental results. It was observed that both the natural frequency and loss factor increased as the area of active electrodes increased.

Steady-state responses in the time domain of the smart plate were experimentally observed by forced vibration tests with both different intensities and areas of electric field applied to an ER fluid. Figure 8 presents the measured responses under the fundamental mode excitation. For each applied pattern of the electric field shown in Figure 8, the comparison of the relative suppressed amplitudes and consumed powers is given in Figure 9. In this plot, the consumed power is normalized with respect to that of full area subject to the electric field of 3 kV/mm. It is shown that for the multielectrode configuration utilized, the suppressed amplitude of a smart plate is more dependent on the location and area ratio of the applied electric field than on the electric field strength.

Table 2. Fundamental frequencies and loss factors of smart composite plate with various energizing areas of 1 kV/mm.

Electric field pattern[a]	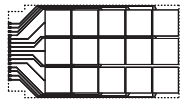		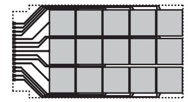		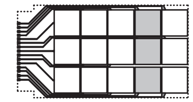	
Exp.: freq. (Hz) L.F. (%)	10.75	4.07	14.68	21.88	11.61	9.28
FEM: freq. (Hz) L.F. (%)	10.60	4.39	15.09	18.59	12.19	11.31
Electric field pattern[a]	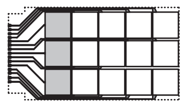		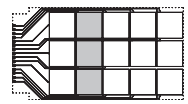		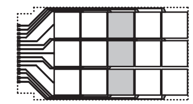	
Exp.: freq. (Hz) L.F. (%)	11.16	4.96	11.51	10.64	11.75	11.44
FEM: freq. (Hz) L.F. (%)	10.73	5.26	11.38	8.75	12.05	11.62
Electric field pattern[a]	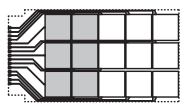		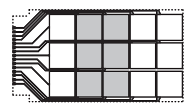		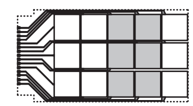	
Exp.: freq. (Hz) L.F. (%)	11.84	11.00	12.40	14.50	12.58	14.08
FEM: freq. (Hz) L.F. (%)	11.49	9.24	12.73	14.16	13.42	15.29
Electric field pattern[a]	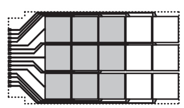		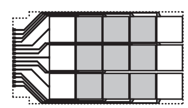		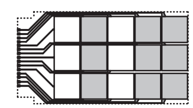	
Exp.: freq. (Hz) L.F. (%)	12.92	15.74	13.94	18.50	13.21	15.86
FEM: freq. (Hz) L.F. (%)	12.84	14.56	14.09	17.62	13.89	15.56
Electric field pattern[a]	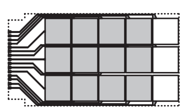		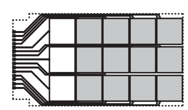		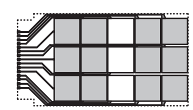	
Exp.: freq. (Hz) L.F. (%)	14.12	26.68	13.48	11.96	14.34	17.62
FEM: freq. (Hz) L.F. (%)	14.22	18.08	14.95	18.08	14.02	16.11

[a] The shaded region indicates applied electric field.

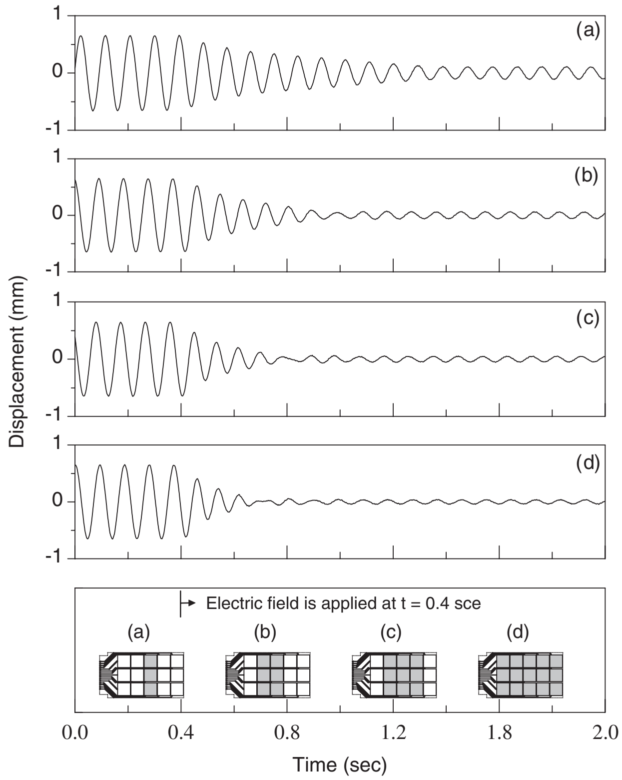

Figure 8. *Steady-state response at different electric field patterns ($E = 2$ kV/mm).*

SEMI-ACTIVE CONTROL

Semi-active control methods have the advantage in suppressing unexpected vibration of the system in terms of reliability, stability, simplicity, and relative cost. Accordingly, a simple semi-active control scheme has been applied. The signal from the laser sensor is fed back into the computer through the DSP board to provide the information on excitation disturbances. Depending on the information from the feedback sensor signal, the control voltages for the ER fluid are determined in the computer through the deflection feedback controller given by MATLAB/Simulink model. Through the formulation of semi-active control schemes and experimental implementation on the condition of full and partial electric activations, both the depressed vibration level and control energy required to suppress the external disturbances were evaluated under the impulse loading. The time response for the semi-active control with a gain of 0.72 is presented in Figure 10. Table 3 presents a comparison of the vibration decay factor and consumed energy for three gains. The vibration decay factor δ given by $\delta\ (\%) = (A_1 - A_2)/A_1 \times 100$ is determined by measuring both the amplitude (A_1) at the impulse excitation and the amplitude (A_2) after 10 complete cycles. It is shown that the consumed

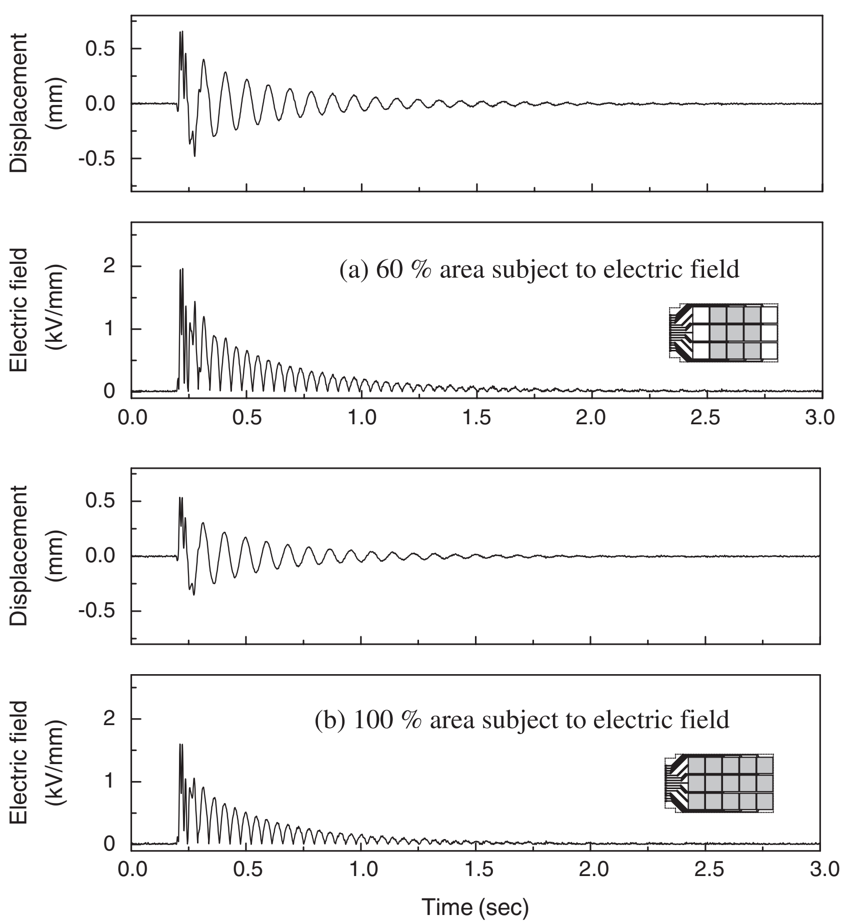

Figure 10. *Transient response with deflection feedback control ($K = 0.72$).*

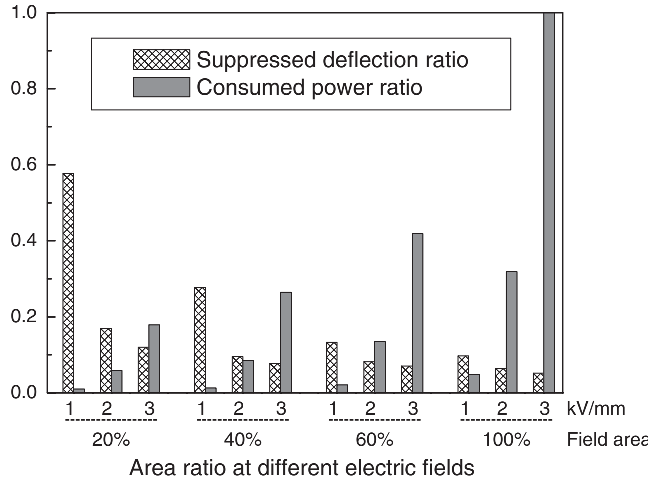

Figure 9. *Comparison of suppressed deflection and consumed power ratio.*

Table 3. Consumed energy and amplitude ratio under impulse excitation of different field patterns.

Vibration control law		Consumed energy (mJ) 60%[a]	Consumed energy (mJ) 100%[a]	Vibration decay factor (%) 60%[a]	Vibration decay factor (%) 100%[a]
Deflection Feedback	$K=0.48$	2.190	5.144	86.4	87.9
	$K=0.72$	7.820	10.130	90.9	91.8
	$K=0.96$	12.865	23.097	93.6	94.6

[a] Field energizing area ratio.

energy of the partial electric activation case is much less than that of the full electric activation while the vibration decay factors are almost the same for two cases.

CONCLUSIONS

The finite element model for the multilayer composite plate containing ER fluid has been developed to study its dynamic characteristics. The effectiveness of refined multielectrodes configuration of the smart plate has been verified through numerical calculation and experimental investigation. It is shown that the vibration response characteristics of the smart structure can be tuned by tailoring the applied field in space. By the optimal use of electrodes, the required energy can be minimized, still maintaining similar damping properties. It is believed that more efficient use of ER fluid is possible when the electric field is concentrated around the area of high shear deformation of ER fluid.

ACKNOWLEDGMENT

This study has been supported by a grant from the National Research Program of the Ministry of Science and Technology, Korea. The authors gratefully acknowledge this support.

REFERENCES

Cho, K.D., Han, J.-H. and Lee, I. 2000. "Vibration and Damping Analysis of Laminated Plates with Fully and Partially Covered Damping Layers," *Journal of Reinforced Plastics and Composites*, 19:1177–1200.

Choi, S.B., Park, Y.K. and Jung, S.B. 1999. "Modal Characteristics of a Flexible Plate Filled with Electrorheological Fluids," *AIAA Journal of Airc*raft, 36:458–464.

Choi, Y., Sprecher, F. and Conrad, H. 1990. "Vibration Characteristics of Composite Beam Containing an Electrorheological Fluid," *Journal of Intelligent Material Systems and Structures*, 1:91–104.

Gandhi, M.V., Thompson, B.S. and Choi, S.B. 1989. "A New Generation of Innovative Ultra-advanced Intelligent Composite Materials Featuring Electro-rheological Fluids: An Experimental Investigation," *Journal of Composite Materials*, 23:1232–1255.

Han, J.-H. and Lee, I. 1997. "Active Damping Enhancement of Composite Plates with Electrode Designed Piezoelectric Materials," *Journal of Intelligent Material Systems and Structures*, 8:249–259.

Mead, D.J. and Markus, S. 1969. "The Forced Vibration of a Three-layer, Damped Sandwich Beam with Arbitrary Boundary Conditions," *Journal of Sound and Vibration*, 10:163–175.

Rahn, C.D. and Joshi, S. 1998. "Modeling and Control of an Electrorheological Sandwich Beam," *ASME Journal of Vibration and Acoustics*, 120:221–227.

Reddy, J.N. 1987. "A Generalization of Two-dimensional Theories of Laminated Composite Plates," *Communications in Applied Numerical Methods*, 3:173–180.

Ross, D., Ungar, E.E. and Kerwin, E.M. 1959. "Damping of Plate Flexural Vibrations by Means of Viscoelastic Laminae," In: Ruzicka, J.E. (ed.), *Structural Damping*, Section 3, ASME.

Yalcintas, M. and Coulter, J.P. 1995. "Electrorheological Material Based Adaptive Beams Subjected to Various Boundary Conditions," *Journal of Intelligent Material Systems and Structures*, 6:700–717.